Effect of Nanoclay Reinforcement on the Property of Rubber Seed Oil Polyurethane Nanocomposites

E. O. Obazee, F. E. Okieimen, A. I. Aigbodion and I. O. Bakare

Abstract Rubber seed oil derived polyol was used in preparing polyurethane nanocomposites by incorporation of surface-modified montmorillonite, MMT, or organoclay, containing 25–30 wt% methyl dihydroxyethyl hydrogenated tallow ammonium) as reinforcement at 1%, 3%, and 5% loading, using hexamethylene diisocyanate (HMDI), 4,4'-methylene-bis(phenylisocyanate) (MDI) to obtain PHM (1, 3, and 5), and PMM (1, 3, and 5), respectively. The physical, mechanical, and morphological properties of the obtained nanocomposites with respect to its neat polyurethane were investigated using x-ray studies (WAXD), nanoindenter (NI), universal testing machine (UTM), Fourier-transform infrared (FTIR) spectroscopy, atomic force microscopy (AFM), and the thermal stability studies determined with thermogravimetric analyzer (TGA). The incorporation of reinforcement led to improvement in some of the properties of the nanocomposites, especially when there was delamination of the MMT in the polymer matrix.

Keywords Rubber seed oil polyol · Polyurethane · Nanocomposites · Modified montmorillonite · Properties

Introduction

Polyurethane is a versatile polymer with wide range of applications [1], such as in sportswear, foams, coating, adhesives, elastomers, and biomedical devices [2, 3]. It fills the gap between plastics and rubber due to its variety of hardness and elastic moduli [4]. It is composed of short, alternating polydisperse blocks of soft and hard segments [5]. Polyurethane has high abrasion resistance, tear strength, flexibility, elasticity, and excellent shock [6]. The properties of polyurethane can be customized

E. O. Obazee (✉) · A. I. Aigbodion · I. O. Bakare
Rubber Research Institute of Nigeria, P. M. B 1049, Benin City, Nigeria
e-mail: eoobazee@gmail.com

F. E. Okieimen
Department of Chemistry & Center for Biomaterials Research, University of Benin, Benin City, Nigeria

The Minerals, Metals & Materials Society (ed.), *TMS 2020 149th Annual Meeting & Exhibition Supplemental Proceedings*, The Minerals, Metals & Materials Series, https://doi.org/10.1007/978-3-030-36296-6_81

apart from varying the stoichiometry, type, and functionality of the reactants, and modification of the polyol, but also, like other polymers by inclusion of nanofillers. The pioneering work on polymer-clay nanocomposites by Usuki et al. [7] ushered in a new window in the science and technology of polymer composite, which has led to intense studies on polymer nanoparticle-filled composites by several authors. For instance, it has been reported [8] that dielectric and magnetic properties have been improved by incorporation of zinc ferrite, mechanical properties have been improved by introduction of calcium carbonate, aluminum hydroxide, kaolin, titanium dioxide, zinc oxide, and silica. Also, improvement of the acoustic properties has been achieved by incorporation of metallic fillers, not to mention modulus, creep resistance, heat resistance, barrier, flame retardancy [9], and luminescence by inclusion of zirconium oxide [10]. However, two of the most used nanofiller [11] are the layered silicate or organoclay (especially montmorillonite, MMT) [12], due to its high aspect ratio and natural abundance [13], and carbon nanotube. Critical requirement in the synthesis of clay-polymer nanocomposites is the good dispersion of the clay in the polymer matrix [14], which is dependent on the purity of the clay mineral and modification [15]. In it natural form, MMT has associated gangue minerals coexisting with it which has to be removed for improvement of its engineering properties, typically elongation, and impact resistance [6]. Among the clay minerals, smectites, especially montmorillonite, have been extensively used to prepare organoclays because of its excellent properties, such as high cation exchange capacity, swelling behavior, adsorption properties, and large surface area [16, 17]. This is aimed at improving its compatibility and to increase the initial interlayer spacing [18], so as to facilitate maximal clay-polymer matrix interaction and dispersibility for optimum properties. Besides, MMT is one of the most used smectite class of aluminum silicate clays in nanocomposites due to its high aspect ratio, environment-friendliness, low cost, and availability. However, the concern and agitations for the preservation of the environment have led to introduction of legislatures on the protection and conservation of the environment. This coupled with the issue of sustainable development and the ever-increasing prices of petrochemicals, which are from finite resource has redirected attention to renewable resources [19–21]. There have been several reports on vegetable oil polyol-based polyurethanes, from soybean oil [2], rapeseed oil, castor oil [22], palm kernel oil, linseed oil, and safflower oil [23].

An earlier study on rubber seed oil polyurethane resin and its bio-composites was via alcoholized RSO (RSO monoglycerides) having lower functionality [24]. Also, polyurethanes obtained from rubber seed oil derived polyol, via epoxidation and ring opening of the formed epoxides have recently been reported elsewhere. In this study, we report the preparation of polyurethane nanocomposites, reinforced by inclusion of organoclay. This is with the hope that the organoclay will impact the rubber seed oil polyurethanes by bringing about improvement in physical, mechanical, and thermal properties of the obtained nanocomposites.

Experimental

Materials

Mechanically expressed rubber seed oil (RSO) was obtained from Rubber Research Institute of Nigeria, Iyanomo Benin City and used as received. Laboratory grade hexamethylene diisocyanates (HMDI), 4,4'-methylene-bis(phenylisocyanate) (MDI), hydrogen peroxide, formic acid, sodium sulfate, sodium chloride, iodine bromide, acetic anhydride, pyridine, dichloromethane, potassium hydroxide, chloroform, crystal violet, toluene, dibutyltindilaurate (DBTDL), and surface-modified montmorillonite containing 25–30 wt% methyl dihydroxyethyl hydrogenated tallow ammonium (organoclay) were obtained from Sigma Aldrich, India.

Structural and Morphology of Polyurethane Nanocomposites

Structural elucidation was determined by FTIR spectroscopy using the Agilent Technologies Cary 660 FTIR attached with attenuated total reflectance (ATR). X-ray diffraction study was carried out with the Rigaku Smartlab Wide Angle X-ray Diffraction (WAXD) machine using CuKα radiation (at $\lambda = 1.54068$ A°) and a Bragg-Brentano geometry, equipped with x-ray generator set at 45 kV tension and 100 mA current, a point proportional detector, and a curve quartz monochromator, a goniometer radius circle of 250 mm was used for examining the crystalline and morphology of the samples. A scanning rate of 0.02°/s over range of 2θ (2°–50°) for one-dimensional X-ray diffraction (XRD) pattern on oriental samples suspended on a glass slide was used for the x-ray studies. The surface morphology of the samples was carried out by atomic force microscopy, using the Bruker Dimension ICON ScanAsyst AFM, and the tapping mode AFM.

Physico-mechanical Properties of Polyurethane and Nanocomposites

Tinius Olsen H50KS Universal Testing machine (using ASTM D 3039, method), 50KN force at a speed of 50 mm/min and gauge length of 12.04, and Hystron TI 950 Triboindenter, with a standard diamond indenter probe, using ASTM E2546-07, were used for determining the mechanical properties and hardness, respectively. The Netzsch STA 449 FI Jupiter thermogravimetric analyzer was used to determine the thermal stability of the samples, at a heating rate of 10 °C min^{-1}, to a temperature of 600 °C, using sample weight between 10 and 14 mg in nitrogen. The degree of swelling of the polymers was carried out by immersing cut-and-weighed size pieces into a solution of toluene, and taking the weight at interval at ambient temperature

until a constant weight was obtained. At this point, the sample was blotted dry with a dry cloth and weighed. Duplicate experiment was carried out for each sample and the average was taken as the final weight [25].

Preparation of Polyurethane Nanocomposites

Mixing of the modified-MMT in RSOP. The rubber seed oil polyol was prepared in our laboratory. The physico-chemical characteristics are given in Table 1 [26]. The required amounts of organoclay (MMT) containing 25–30 wt% methyl dihydroxyethyl hydrogenated tallow ammonium) to give 1, 3, and 5 wt% was used with moisture-free polyol (RSOP) dissolved in toluene in a three-necked flask according to the method of Sari et al. [19] with modification. The mixture was dispersed using a sonicator at room temperature for two hours, to effect sufficient mixing of the organoclay and polyol to give MMT-polyol mixtures (at 1, 3, and 5% loadings). The percentage of MMT added is with respect to the amount of RSOP.

Into the three-necked flask containing the homogeneous uniformly dispersed MMT-polyol mixtures, as in above, under reflux and fitted with nitrogen gas inlet was charged DBTDL catalyst (1%) and toluene. This was stirred for some time to enable proper mixing in an inert atmosphere. Then the calculated amount of HMDI required to give NCO/OH ratios of 1.0 was charged into the reactor and stirred for about two minutes and de-gassed, and poured into a mold and cured for two hours at 60 °C, and finally cured for about twelve hours at 100 °C to obtained the respective MMT-polyurethane nanocomposites; from HMDI (samples PHM1, PHM3, and PHM5) and from MDI (samples PMM1, PMM3, and PMM5), having 1, 3, and 5% MMT loading, respectively.

Table 1 Physico-chemical properties of RSOP

Properties	HRSO
Colour	Orange–yellow
Density	1.019
AV (mg KOH g^{-1})	14.733
SV (mg KOH g^{-1})	239.17
IV ($gI_2 100\ g^{-1}$)	9.240
HV (mg KOH g^{-1})	203.47
Oxirane content (%)	0.402
Mn (g mol^{-1})	1014.68*
Fn	3.7524

Results and Discussion

Structure and Morphology of Polyurethane Nanocomposites

The FTIR spectra of HMDI polyurethane (PUH) and derived nanocomposites (PHM1, 3, and 5), and MDI polyurethane (PUM) and derived nanocomposites (PMM1, 3, and 5) are shown in Fig. 1a, b. From the spectra, the similarity of the pristine polyurethanes and derivative polyurethane nanocomposites is revealed. The typical donor N–H and acceptor C = O stretching absorption bands of polyurethane at 3300–3360 cm^{-1} and 1695–1735 cm^{-1}, respectively, based on the extent of the H-bonding in the polyurethanes. In the carbonyl region, the presence of the associated and non-associated stretching bands, which represents the level of H-bonding and free or non-hydrogen bonding within the urethanes structures, are visible. It is observed that the peaks of the H-bonded C = O are more intense and broad, which also reflects the level of inter-molecular activities in the network. Also present is the aromatic peak (for the MDI derivatives), the asymmetric and symmetric stretching absorption bands of −CH, etc.

X-ray diffraction (XRD): The morphology of the polyurethanes and respective nanoclay reinforced polyurethane nanocomposites (PHMs and PMMs) at 1, 3, and

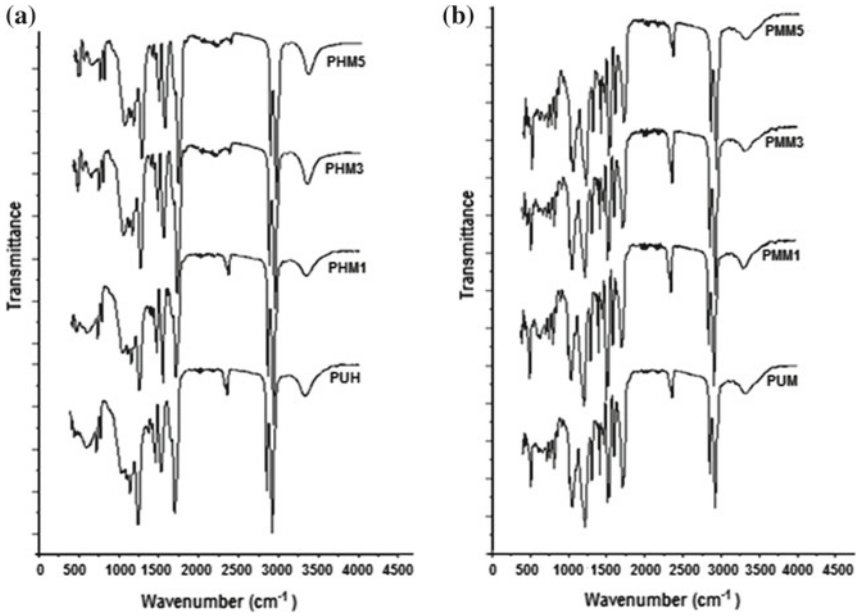

Fig. 1 FTIR **a** of HMDI polyurethane and nanocomposite, **b** MDI polyurethanes and nanocomposite

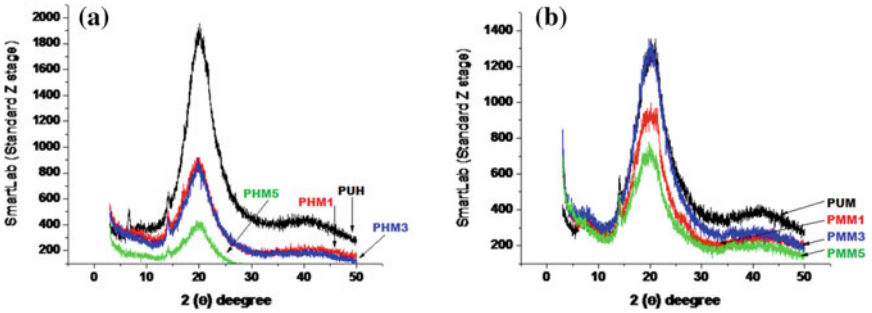

Fig. 2 XRD of **a** HMDI polyurethane and nanocomposites, **b** MDI polyurethane and nanocomposites

5% loading were examined with the WAXD, Fig. 2a, b. All polyurethane nanocomposites like their neat polymer are mainly amorphous in nature as evidenced in their halo characteristic peaks at 20° and 40° in the 2(θ) degree range. In Fig. 2b, the diffractions of MMT and those of PUH, PUM, and nanocomposites are combined, and it shows the basal reflection peak at about 4.7° in the 2(θ) degree range of the organoclay. Of all the nanocomposites only PHM1 showed a little hump at about 4°–6.8° angular range of reflection of the organoclay, implying that the polymer was inserted in the interlayer gallery of the nanofiller leading to intercalated nanocomposites morphology. Whereas, in the diffractograms of PHM3 and PHM5, it is observed that there is the absence of the basal reflection peak of the organoclay filler at about its angular reflection range, which implies successful separation of the nanofiller into individual layer in the continuous polymer matrices. This implies the formation of delamination of the organoclay to form exfoliated nanocomposites structures in PHM3 and PHM5. Also, in the PUM derived nanocomposites, all were found to show absence of the basal reflection peaks of the organoclay, which implies sufficient mixing of MMT in the polymer matrices, such that the nanoclay individual particles are successfully delaminated or exfoliated. It is known generally that when polymer–clay interactions are optimized there is the high tendency to form delaminated or exfoliation mixing, which leads significantly to improvement in mechanical and physical properties, compared to when intercalation is formed [27, 28] (Fig. 3).

Mechanical Properties

The mechanical properties of the polyurethane and nanocomposites are depicted in Table 2. The hardness of the polyurethane nanocomposites increased with

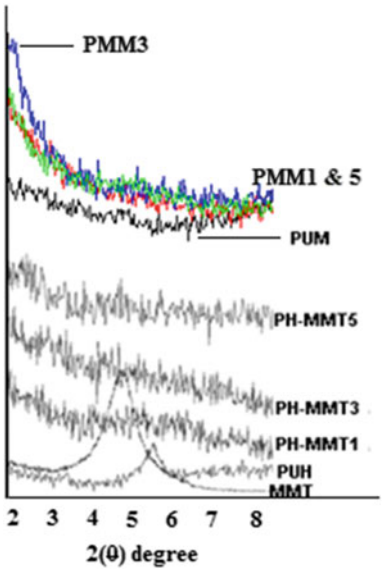

Fig. 3 All XRDs at MMT basal peak range

Table 2 Physico-mechanical properties of polymer and nanocomposites

Sample	Young's modulus (MPa)	Average hardness (MPa)	Tensile strength (MPa)	Elongation @ break (MPa)	Ultimate true stress (MPa)	Yield stress (MPa)	Swelling @ 30 °C (%)
PUH	15.97	1.399 ± 0.01	2.09	187	5.93	2.09	1.58
PHM1	12.6	1.573 ± 0.02	2.48	95.6	5.32	0.516	1.65
PHM3	81.26	4.215 ± 0.02	3.06	159	7.87	3.06	1.56
PHM5	102.24	9.724 ± 0.01	6.68	42.2	9.34	6.68	1.54
PUM	1,963.10	60.507 ± 0.02	5.17	161	12.6	5.17	1.51
PMM1	2,709.70	68.446 ± 0.02	6.67	74.7	10.6	6.62	1.5
PMM3	2,931.40	100.64 ± 0.01	7.45	345	16.3	7.45	1.43
PMM5	2,835.60	178.452 ± 0.02	13.4	287	54.4	10.6	1.38

nanoreinforcement with respect to the pristine polymer PUH, resulting to an increment of about 12.45%, 201.9%, and 595.1% in PHM1, PHM3, and PHM5, respectively, and 13.12, 66.32, and 194.9% in PMM1, PMM3, and PMM5. The loading-unloading curves obtained from the nanoindenter are presented in Fig. 4a, b, and reflects an increment in hardness with nanofiller loading.

The tensile strength of the polyurethanes and nanocomposites obtained, with the stress–strain curves in Fig. 5a, b, also increased with organoclay loading. This represents about 18.66% increment in PHM1, 46.411% and 229.2% in PHM3 and PHM5, with 1%, 3%, and 5% MMT reinforcement, respectively. Also the same pattern was

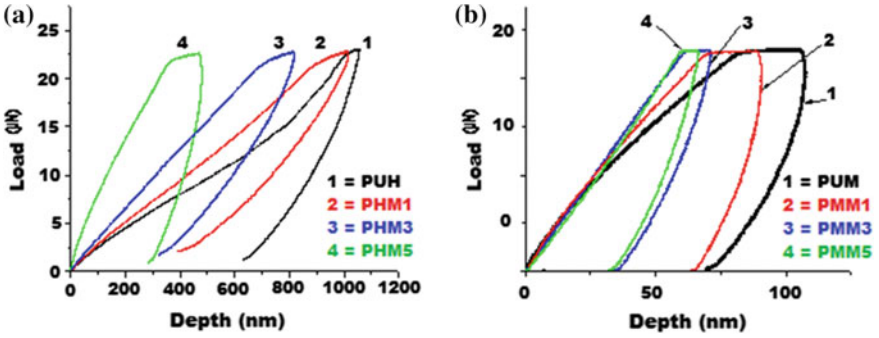

Fig. 4 Loading-unloading curves of **a** HMDI and polyurethane, **b** MDI polyurethane and nanocomposite

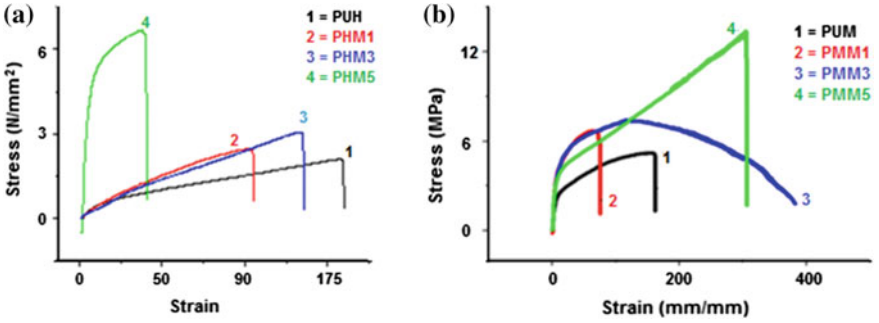

Fig. 5 Stress–strain curves of **a** HMDI poyurethane and nanocomposites, **b** MDI polyurethane and nanocomposites

observed in PMM1, PMM3, and PMM5 of 29.015%, 44.10%, and 159.18% increase in tensile strength, respectively, with organoclay reinforcement.

The young modulus were similarly improved as the nanofiller loading increased except in PHM1, were 26.74% reduction was recorded. PHM3 and PHM5 increased by 408.8% and 540.2%, respectively. Also, PMM1, PMM3, and PMM5 showed an increment of 38.03%, 49.35%, and 44.41%, respectively, from PUM1. The observed decrease in modulus of PHM 1 could be explained by the fact that the interactions at the interphases of the layered galleries of the nanofiller and the polymer matrix was not at a maximum and hence did not result to a delaminated morphology, which could have brought them to shorter distances and facilitate better interaction. The values of PUM and it nanocomposites are far higher than those of PUH and its nanocomposites, due to the presence of aromatic rings, increased cross-linked density and higher level of hydrogen bonding, which contributes to the stiffening and, thus, resulted to general hardness. The elongation at break was observed to decrease as expected, but not irregularly. Going from the unfilled PUH (187%), elongation at break decreased to 95.9% in PHM1, 159% in PHM3 and 42.2% in PHM5 (see Fig. 6a). However, as

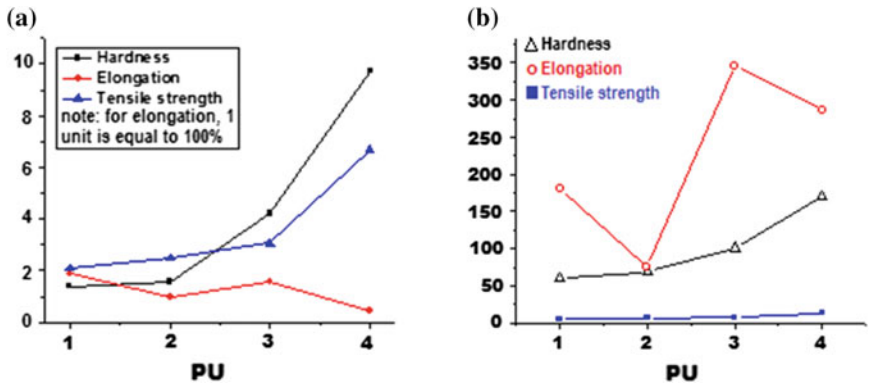

Fig. 6 Changes in properties with filler loading **a** HMDI polyurethane and nanocomposites, **b** MDI polyurethane and nanocomposites

seen in Fig. 6b, there is an initial decrease from the unfilled PUM (161%) to 74.7% in PMM1, and an unprecedented increase to 345 and 287% in PMM3 and PMM5. The reasons for the disparities in the elongation at break could not be appropriately linked to increment in nanoreinforcement. But it is suggestive that the nanoclay effected plasticity in the two latter cases (PMM3 and PMM5).

The ultimate true stress and yield stress were observed to have decreased in PHM1 and later increases in PHM3 and PHM5. This was also the case for PMM1, decreasing initially from PUM1, and subsequently increases in PMM3 and PMM5 for the ultimate true stress. But for the yield stress the values increased with increasing organoclay loading.

The results of the degree of swelling are compared graphically in Fig. 7, with an increase recorded in PHM1 of about 13%, and a decrease in PHM 3 and PHM5 of about 2.2% and 6.0%, respectively. There was an observed decrease with loading

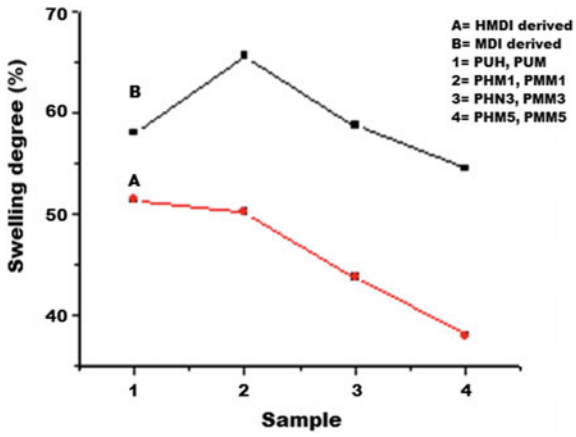

Fig. 7 Degree of swelling of polyurethanes and nanocomposites

from PUM to PMM1 and down to PMM5. Therefore, with the exception of PHM1 (intercalated nanocomposite), it means that there was a decrease in the degree of swelling in all the exfoliated nanocomposites, due to decrease in its barrier property, which increased in the other nanocomposites. It implies that the organoclay sheet-like platelets did not bring to bear the effect of it high surface area in PHM1 as it did in the other nanocomposites. In comparison, the PUH derived nanocomposites had higher values than those derived from PUM.

Thermal Stability

The onset of degradation is generally low for these polyurethane and occurs at approximately between 130 and 210 °C.

The low thermal stability of urethane linkages is mainly responsible for the low degradation temperature of polyurethane and is due to low dissociation energies of chemical bonds present in urethane linkage structure [29]. The low values of onset in PHM1 and PMM3 could be as a result of presence of moisture or any extraneous material. The results obtained from the TGA are tabulated in Table 3, and it reveals marginal changes in some of the polyurethane nanocomposites as shown in the thermograms in Fig. 8a, b for the PUH/PHMs and PUM/PMMs, respectively. The thermogram of PUH and its nanocomposites passed through two decomposition steps, unlike the PUM and PMMs, which had three decomposition steps. The intermediate steps in PUM and its nanocomposites are due to the aromatic rings present in the MDI monomer. The temperature of first step of degradation showed a decrease from the unfilled polyurethane, PUH, to PHM1, and an increment in PHM3 and PHM5 nanocomposites which both had the same values. In the second or final stage of degradation there is improvement in PHM1, which had the highest temperature, followed by PHM3, while PHM5 had the lowest temperature.

For PUM and its nanocomposites, there was increase in temperature at 1 and 5% (PMM1 and PMM5) organoclay loading from the unfilled polyurethane (PUM) in

Table 3 Thermal properties of polyurethanes and nanocomposites

Sample	Onset	1st step	2nd step	3rd step
PUH	202	298	515	
PH-MMT1	130	297	518	
PH-MMT3	199	301	515	
PH-MMT5	192	301	505	
PUM	205	297	430	520
PM-MMT1	210	301	440	515
PM-MMT3	175	297	436	538
PM-MMT5	210	301	436	538

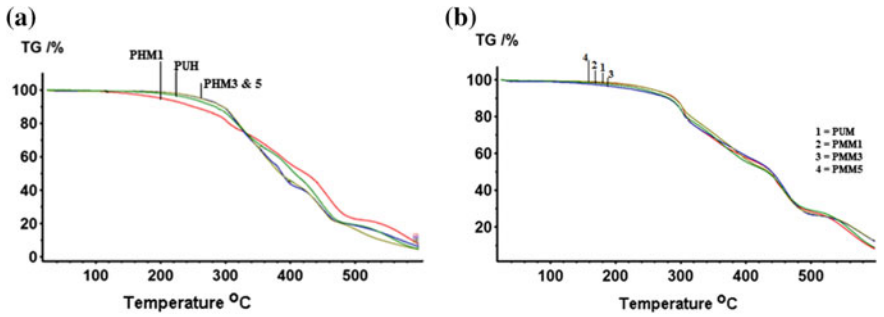

Fig. 8 TGA of **a** HMDI polyurethane and nanocomposites, **b** MDI polyurethane and nanocomposites

the first step of degradation, while PMM3 showed no temperature change. In the second step of degradation, there is an observed increase in all the nanocomposites compared to the unfilled polyurethane (PUM) with PMM1 (1% organoclay loading) having the highest temperature change. However, at the third step, PMM3 and PMM5 had the same and highest degradation temperatures. In general, marginal changes are observed in the thermal stability of the polymer nanocomposites obtained from the aliphatic (HMDI) isocyanate without any clear and defined pattern. But in the aromatic (MDI) isocyanate derived nanocomposites the improvement was somewhat with organoclay loading.

The result obtained from this investigation has revealed that exfoliated polyurethane nanocomposites had better property improvement than the intercalated nanocomposite (PHM1). The generalization that delaminated or exfoliated systems, which has higher phase homogeneity and interactions [30], leads to improved mechanical properties, especially strength and Young's modulus, than intercalated systems [31], is confirmed in this study. Insufficient interaction between polymer matrix and nanofiller at interphase level could be the reason for the lesser mechanical properties of the intercalated nanocomposites. This can be adduced to the strong tendency to agglomerate as a result of the big contact surfaces exhibited by sheet-like nanoparticles, which probably was not sufficiently dispersed at the point of inclusion of organoclay unto the polyol. Conversely, successful delamination of the organoclay facilitates the best improvement as a result of the larger surface area and aspect ratio of the organoclay [32] as seen in PHM3 and 5, and PMM1, 3, and 5.

Conclusion

In this study, rubber seed oil derived polyol was successfully used in preparing organoclay reinforced polyurethane nanocomposites, with varied content of nanofiller. The morphology of the nanocomposites produced was an intercalated and delaminated systems as indicated by the WAXD results. The mechanical properties of

the nanocomposites all showed improvement with respect to their unfilled or neat polymers, however, with the exfoliated nanocomposites having better properties as compared to the intercalated nanocomposite. Also reinforcement of the polyurethane with organoclay also led to some improvement in thermal stability.

Acknowledgements The authors wish to acknowledge the Director of Indian Institute of Technology Mandi, Himachal Pradesh, India, for providing the laboratory, chemicals, and the research internship for this study, and the Executive Director of Rubber Research Institute of Nigeria for the leave granted EOO.

References

1. Sardon H, Pascual A, Mecerreyes D, Taton D, Cramail H, Hedrick JL (2015) Synthesis of polyurethanes using organocatalysis: a perspective. Macromol 48(10):3153–3167. https://doi.org/10.1021/acs.macromol.5b00384
2. Lligadas G, Ronda RC, Galia M, Biermann U, Metzger JO (2006) Synthesis and characterization of polyurethane from epoxidized methyl oleate based polyether polyol as renewable resources. J Polym Sci Part A Polym Chem 44:634–645
3. Maji PK, Guchhait PK, Bhowmick AK (2009) Effect of nanoclays on physico-mechanical properties and adhesion of polyester-based polyurethane nanocomposites: structure–property correlations. J Mater Sci 2009(44):5861–5871
4. Pashaei S, Hosseinzadeh S (2014) Modification in physical properties of organo clay filled polyurethane nanocomposites. Polym Sci Ser A 56(6):874–883
5. Schollenberger SC (2001) In: Bhowmick AK, Stephens HL (eds) Handbook of elastomers, 2nd edn. Marcel Dekker Inc., USA
6. Thuc CNH, Cao HT, Nguyen DM, Tran MA, Duclaux L, Grillet A-C, Thuc HH (2014) Preparation and characterization of polyurethane nanocomposites using vietnamese montmorillonite modified by polyol surfactants. J Nanomater, Article ID 302735, 1–11. http://dx.doi.org/10.1155/2014/302735
7. Usuki A, Kojima Y, Kawasumi M, Okada A, Fukushima Y, Kurauchi T, Kamigaito O (1993) Synthesis of nylon 6-clay hybrid. J Mater Res 8:1179–1184
8. Nunes RCR, Fonseca JLC, Pereira MR (2000) Polymer–filler interactions and mechanical properties of a polyurethane elastomer. Polym Test 19:93–103
9. Lu Y, Larock RC (2006) Novel biobased nanocomposites from soybean oil and functionalized organoclay. Biomacromol 7:2692–2700
10. Ryszkowska J, Zawadzak EA, Łojkowski W, Opalińska A, Kurzydłowski KJ (2007) Structure and properties of polyurethane nanocomposites with zirconium oxide including Eu. Mater Sci Eng C 27:994–997
11. Gacitua WE, Ballerini AA, Zhang Jinwen (2005) Polymer nanocomposites: synthetic and natural fillers. Maderas Ciencia Y Technol 7(3):159–178
12. Chu C-C, Chiang M-L, Tsai C-M, Lin J-J (2005) Exfoliation of montmorillonite clay by mannich polyamines with multiple quaternary salts. Macromolecules 38:6240–6243
13. Wang C, Ding D, Wua Q, Liu F, Wei J, Lu R, Xieb H, Chen R (2014) Soy polyol-based polyurethane modified by raw and silylated palygorskite. Ind Crops Prod 57:29–34
14. Konwar U, karak N, Mandal M, Mesuaferrea L (2009) Seed oil based highly thermostable and biodegradable polyester/clay nanocomposites. Polym Degrad Stab 94:2221–2230
15. Shiraz NZ, Enferad E, Monfared A, Mojarrad MA (2013) Preparation of nanocomposite based on exfoliation of montmorillonite in acrylamide thermosensitive polymer. ISRN Polym Sci, Article ID 280897, 1–5. http://dx.doi.org/10.1155/2013/280897

16. Alexandre M, Dubois P (2000) Polymer-layered silicate nanocomposites: preparation, properties and uses of a new class of materials. Mater Sci Eng R 28:1–63
17. de Paiva LB, Morales AR, Díaz FRV (2008) Organoclays: properties, preparation and applications. Appl Clay Sci 42:8–24
18. He H, Ma L, Zhua J, Frost RL, Theng BKG, Bergaya F (2014) Synthesis of organoclays: a critical review and some unresolved issues. Appl Clay Sci 100:22–28
19. Sari MG, Ramezanzadeh B, Shahbazi M, Pakdel AS (2015) Influence of nanoclay particles modification by polyester-amide hyperbranched polymer on the corrosion protective performance of the epoxy nanocomposites. Corros Sci 92:162–172
20. Fridrihsone A, Stirna U, Lazdina B, Misane M, Vilsone D (2013) Characterization of polyurethane network structure and properties based on rapeseed oil derived polyol. Eur Polym J 49:1204–1214
21. Pechar TW, Wilkes GJ, Zhou B, Lou N (2007) Characterization of soy-based polyurethane networks prepared with different diisocyanates and their blends with petroleum-based polyol. J Appl Polym Sci 106:2350–2362
22. Petrovic ZS, Yang L, Zlatanic A, Zhang W, Javni I (2007) Network structure and properties of polyurethanes from soybean oil. J Appl Polym Sci 105:717–2727
23. Kong X, Narine SS (2008) Physical properties of sequential interpenetrating polymer network produced from canola oil-based polyurethane and poly(methyl methacrylate). Biomacromol 9:1424–1433
24. Lyon CK, Garrett VH, Frankel EN (1974) Rigid urethane foams from hydroxymethylated castor oil, safflower oil, oleic safflower oil, and polyol ester of castor acid. J Am Oil Chem Soc, 331–334
25. Okieimen FE, Bakare IO (2007) Rubber seed oil-based polyurethane composites, fabrication and properties evaluation. Adv Mater Res 18–19:233–239
26. Ferrer CC, Babb D, Ryan AJ (2008) Characterization of polyurethane networks based on vegetable derived polyol. Polymer 49:3279–3287
27. Obazee EO (2018) Biobased polymers and nanocomposites from modified rubber seed oil. PhD Thesis, University of Benin, Benin City
28. Varlot K, Reynaud E, Kloppfer MH, Vigier G, Varlet J (2001) Clay–reinforced polyamide: preferential orientation of the montmorillonite sheets and the polyamide crystalline lamellae. J Polym Sci, Part B Polym Phys 39:1360–1370
29. Chin I-J, Thurn-Albrecht T, Kim H-C, Russell TP, Wang J (2001) On exfoliation of montmorillonite in epoxy. Polymer 42:5947–5952
30. Ionescu M (2005) Chemistry and technology of polyols for polyurethanes, Chap. 17. Rapra Technology Limited, UK
31. Koo JH (2006) Polymer nanocomposites: processing, characterization, and applications. McGraw Hill, NY, pp 1–20, 61–76
32. Jahanmardi R, Kangarlou B, Dibazar AR (2013) Effect of organically modified nanoclay on cellular morphology, tensile properties, and dimensional stability of flexible polyurethane foams. J Nanostruct Chem 3(82):1–6